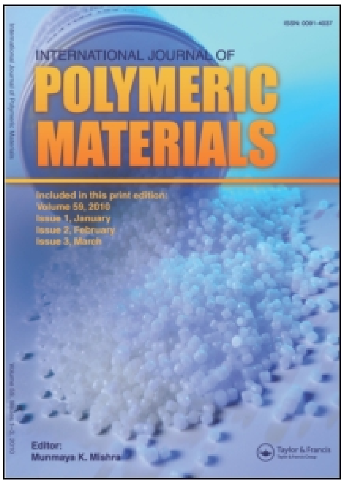

International Journal of Polymeric Materials
Publication details, including instructions for authors and subscription information:
http://www.informaworld.com/smpp/title~content=t713647664

Thernial Expansivity and Relaxational Behavior of Amorphous Polymers at Low Temperatures

James M. Roe[a b]; Robert Simha[a]
[a] Department of Macromolecular Science, Case Western Reserve University Cleveland, Ohio [b] Styrene Molding Polymers R & D, The Dow Chemical Company, Midland, Michigan.

To cite this Article Roe, James M. and Simha, Robert(1974) 'Thernial Expansivity and Relaxational Behavior of Amorphous Polymers at Low Temperatures', International Journal of Polymeric Materials, 3: 3, 193 — 227

To link to this Article: DOI: 10.1080/00914037408072353

URL: http://dx.doi.org/10.1080/00914037408072353

Intern. J. Polymeric Mater., 1974, Vol. 3, pp. 193–227

Printed in Reading, England

Thermal Expansivity and Relaxational Behavior of Amorphous Polymers at Low Temperatures

JAMES M. ROE† and ROBERT SIMHA‡

Department of Macromolecular Science, Case Western Reserve University
Cleveland, Ohio 44106

(*Received September 10, 1973*)

A linear dilatometer is described. It differs from one previously employed by us by making possible the use of thin specimens. The linear thermal expansivity is obtained in the range $7 \leq T \leq 350$ K with an accuracy of $\pm 1 \times 10^{-6}(\mathrm{K})^{-1}$. Three widely different families were studied, namely polystyrene and two poly(methyl styrenes), four tough so-called engineering plastics and six esters of poly(methacrylic acid), including the series of five to eight-membered saturated ring polymers. In all but one of these systems, at least one sub-T_g relaxation region is observed. Excellent agreement between these and relaxations detected by dynamic techniques is obtained, with appropriately enhanced resolution by the slower dilatometry. In order to make meaningful comparisons we adopt a semi-empirical method for computing the temperature-frequency shift. This, it is shown, can be based on an Arrhenius equation with a universal value of the pre-exponential factor. The effective frequency of the dilatometer turns out to be about 10^{-3} Hz. Relaxation processes associated with sidechain motions are dilatometrically more intense than others, as seen by a comparison of the engineering plastics with the cyclo-methacrylates. Finally we apply the low temperature equation of state, derived and discussed by Nanda and us in connection with the present experimental data, to our earlier measurements. These involved primarily homologous series of alkyl methacrylates and vinyl ethers. Again a low temperature mastercurve, identical with that for our present polymers, results. Exceptions in the pattern for some methyl containing polymers are discussed.

1 INTRODUCTION

In the past 20 years or so, the physical properties and relaxations of polymers have been studied by a wide variety of techniques in attempts to

---

†Present address: Styrene Molding Polymers R & D, The Dow Chemical Company, Midland, Michigan.

‡To whom correspondence should be directed.

correlate changes in physical properties with known transitions and to determine the molecular origin of these relaxations. Dilatometry, a frequently employed tool for investigation of the glass transition, has not been fully exploited as a technique for study of the more subtle secondary relaxations found below T_g. This lack of popularity is due in part to difficulties in both the obtainment and analysis of low temperature data. In recent years, significant progress has been made in both areas and dilatometry has become a sensitive tool for the study of sub-T_g relaxations.

Simha and his colleagues have previously measured the expansivities of numerous polymers in the temperature range $20\ \mathrm{K} < T < T_g$.[1-6] These studies included a homologous series of poly(alkyl methacrylates) and poly (vinyl alkyl ethers) as well as some crystalline polymers. Generally they found that the dilatometer revealed several sub-T_g relaxations where dynamic techniques were able to detect only a single damping maximum. This enhanced resolution is due to the inherent low frequency of the dilatometric method.

More recently, we have presented a low temperature equation of state which is based on a cell model in the harmonic approximation.[7] The theory was compared with the low temperature expansivity of a number of polymers and good agreement was found between theory and experiment in regions where relaxations did not occur. Moreover, a low temperature principle of corresponding states ensued from these considerations, since the reduced quantum temperature turns out to have a universal value for the widely differing polymeric structures analyzed.

The purposes of this paper are: First, the description of a cryogenic dilatometer, differing in some respects from earlier designs. Second, the study of a series of structurally very diverse amorphous polymers. Third, the correlation of dilatometrically and dynamically obtained relaxation regions. Finally, we compare the thermal expansivities with the predictions of the low temperature theory for several of the earlier systems.

2 EXPERIMENTAL

2.1 Cryogenic dilatometer

The primary equipment used in these investigations is a linear quartz type dilatometer, designed to operate in the temperature range 4.2 to 350 K. This style of dilatometer has been used successfully and described by several previous authors.[3,4,8] Our design differs from previous ones in that it features a counter-balanced inner quartz tube which holds the sample in very slight tension. This feature allows the use of thin specimens.

The quartz dilatometer consists of three subsystems whose functions are to measure the length change and temperature of the specimen, to heat it at the proper rate and also to assure a low thermal gradient in the sample area. The instrument design and construction will be discussed in terms of these subsystems in the following.

The sample is placed in a sample chamber whose temperature can be closely controlled, and the actual length change is transmitted via quartz tubes to a transducer which is kept at ambient temperature. The details of this construction are shown in Figures 1 and 2. The sample (A) is held by the upper (B) and lower (C) Invar sample grips. These are held in turn respectively by

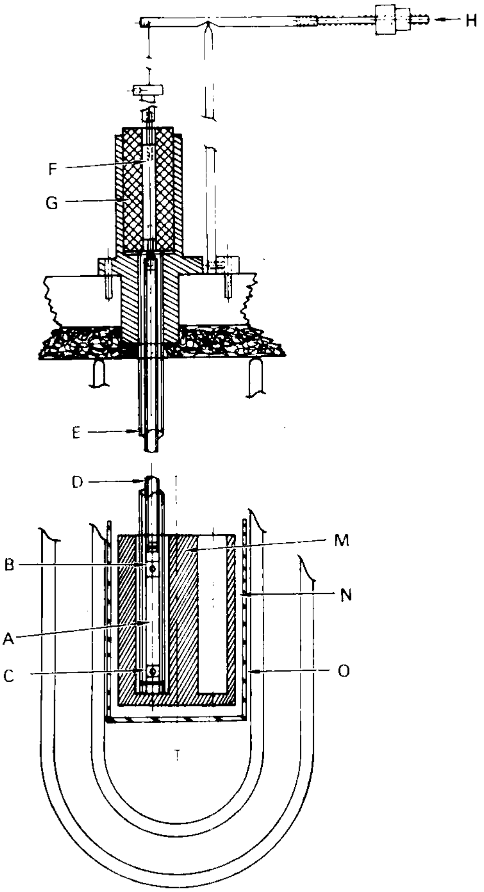

FIGURE 1 Cryogenic dilatometer (schematic). [A] sample; [B] upper grip; [C] lower grip; [D] inner support tube; [E] outer support tube; [F] LVDT core; [G] LVDT coil; [H] counter balance weight; [M] heater block; [N] insulation; [O] aluminum heat shield cylinder.

an inner (D) and an outer support tube (E), which are made mainly of fused quartz. However, the lower three inches of the outer support tube consist of Invar because of the necessity of machining slots in it to allow heat transfer and for holding the lower grip. This sample holding system rests in one of the wells of the heater block (M). Since the bottom sample grip (C) joins the sample to the outer sample support tube, any motion of the upper sample grip relative to the outer sample support tube must be due to differences in thermal expansion between the sample and the Invar of the lower part of the outer sample

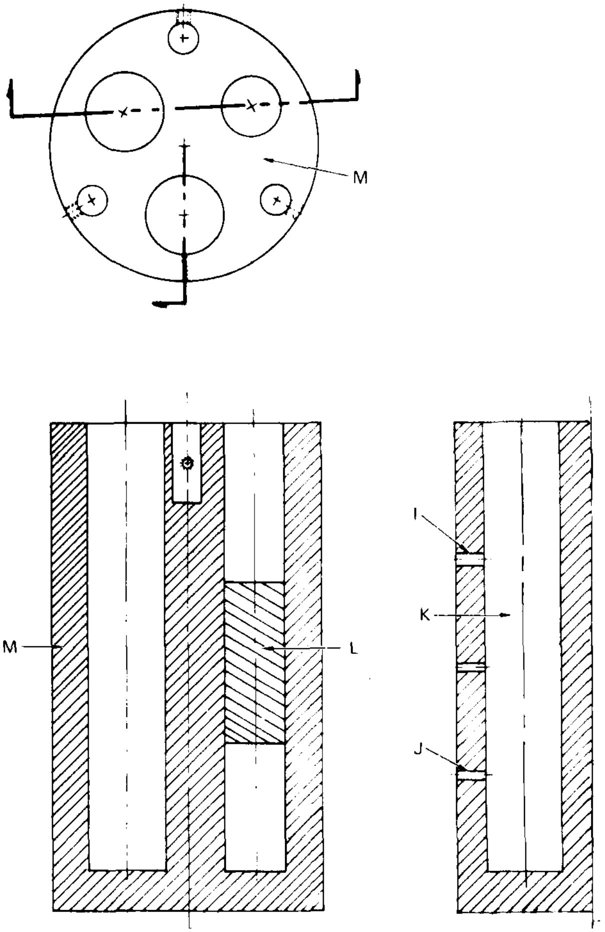

FIGURE 2 Heater block assembly. [I] Upper helium referenced thermocouple; [J] lower helium referenced thermocouple; [K] ice-water referenced thermocouple; [L] cartridge heater; [M] heater block.

support tube. The thermal expansion of Invar is much smaller than that of most polymers and could be ignored in most cases. However, as will be seen later, even this small effect can and has been taken into account. The length change of the sample is transmitted to the linear transducer by the inner (C) and outer (D) quartz support tubes which are connected respectively to the core (F) and coil (G) of the linear transducer (LVDT). Since these tubes have the same length and are made of the same low thermal expansion material, it is assumed that their lengths do not change relative to each other, even though their temperatures and actual lengths do change during the course of the experiment. This assumption is valid as long as the temperature of the sample is varied slowly enough so that both of the tubes are at the same temperature at each level between the sample and the LVDT.

The change of the sample length is measured by a Model 300D Daytronic linear variable differential transducer, which is calibrated so that a full scale deflection corresponds to 0.0100 inch. The signal is amplified by a Model 860-4300 Sanborn low level amplifier and is fed to a Hewlett Packard Model 3439A voltmeter which can detect voltages to $\pm 0.01\%$. This makes it possible to detect length changes of 1×10^{-6} inch in a sample 1.5 inches of length.

As has been mentioned earlier, the sample is held in very slight tension, which is the most stable force transmitting configuration for a thin film. This supporting tension is provided by a counter balance (H) which suspends the inner support tube through the core of the LVDT and a monofilament nylon line. The counter weight is adjustable so that it provides a tensile force of 10^5–10^6 dynes/cm^2 on the specimen. Such a force causes a negligible extension of the polymer in the glassy state. However, viscous flow can and does occur above T_g, which limits the use of this equipment to the glassy region.

The temperature of the sample is measured by two sets of copper constantan thermocouples. As is shown in Figure 2, these thermocouples are actually located in a dummy sample well which is geometrically identical with the real sample well. This construction is used so that it is not necessary to move the thermocouples in and out of the sample well each time a sample is changed, thus making sample installation more convenient and avoiding any additional source of error.

In the low temperature region ($T < 100$ K), the temperature is monitored by the thermocouples (I and J) as shown in Figure 2. These are referenced to the liquid He in the bottom of the flask and are connected in series for maximum sensitivity. At higher temperature (80–350 K), when the He has evaporated from the inner Dewar flask (see Figure 1), the temperature is measured by the thermocouple (K) which is referenced to an external ice junction. The signals from the thermocouples are amplified by the Sanborn linear amplifier and fed to the digital voltmeter. A difference in voltage of 1×10^{-6} volts can thus be detected by this system. An examination of thermocouple EMF tables indicates that this corresponds to an error of less than 0.1 K above 10 K and less than 0.2 K for T less than 10 K.[9]

The sample is heated primarily by the cartridge heater (L) which sits in the third well of the heater block (M). The heater block is surrounded by insulation (N) and an aluminium cylinder (O) which has a wire wound resistance heater (see Figure 1). This heater serves as a shield so that there is a minimum temperature gradient between the heater block and its immediate surroundings. The temperature of this exterior cylinder is monitored by a thermocouple placed against its inner wall, and it is kept to within 1° of the temperature of the heater block.

The entire heater area is surrounded by a double Dewar system. The inner Dewar contains liquid He for cooling to 4.2 K and to provide a reference temperature for the low temperature thermocouple system. The outer Dewar contains liquid N_2 which reduces the thermal gradient to the outside. This helps to slow the natural heating rate of the equipment. The sample area is insulated from heat leaks from above by an 18-inch polyethylene foam plug.

2.2 Calibration and testing

The voltmeter is calibrated by an internal standard so that it reads 1 volt full scale with an accuracy of 1×10^{-4} volts. The linear amplifier was then calibrated by feeding in a precisely known voltage from a Leeds and Northrop K3 potentiometer and adjusting the gain until the output to the voltmeter was exactly 100 times as great. It was found that the amplifier voltmeter system used to measure the voltage of the thermocouples and LVDT was linear to better than 0.05% and drifted less than 0.1% from calibration to calibration.

The LVDT was calibrated by displacing the core of the transducer by a known amount by means of a precision micrometer and adjusting the output signal so that a length change of 0.01000 inch corresponded to a reading of 1.0000 volts on the voltmeter. This made it possible to detect length changes of 10^{-6} inch. The linearity of this equipment was better than 0.1% and the drift between calibrations was less than 0.1% which was the limit of calibration.

From the known errors in the length and temperature measurements, it is possible to compute the most probable error in the thermal expansion. To make such calculations, it is necessary to assume that there are no errors due to thermal gradients along the quartz support tubes and that the thermal expansion of Invar can be neglected compared to that of polymers. Therefore it was thought that the typical error could be better estimated by measuring a material of known thermal expansion. Copper was chosen as a standard material because very good data are available from the National Bureau of Standards[10] and because it has been shown that the thermal expansion of copper is relatively insensitive to its origin so long as it is pure and oxygen free.[11]

Figure 3 compares the smoothed NBS data with the values derived from the quartz dilatometer. If one takes the solid line through the solid points as representative of the thermal expansion of copper and compares this with the values obtained at the NBS, one finds a systematic deviation of 1-2 × 10^{-6} in/in/°K. This systematic deviation, which is plotted in the upper part of Figure 3, is considered to be inherent in the equipment, for in fact the instrument is measuring the difference between the thermal expansion of Invar and the sample material. To check the feasibility of the assumption that the error in the thermal expansion may be due to the expansion of the Invar in the outer support tube, the thermal expansion of Invar[11] was compared with the systematic deviation. It was found that the difference between the two was not greater than 1 × 10^{-6}/°K above 30 K. The greater deviation below 30 K is due to differences in temperatures between the two quartz tubes which results

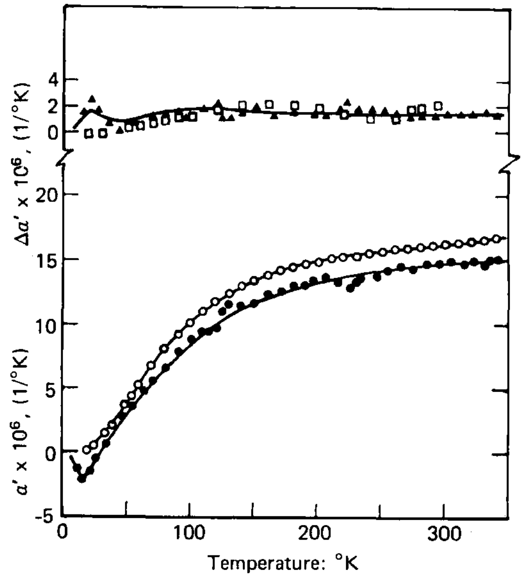

FIGURE 3 Thermal expansion of copper. ○—NBS data[9]; ●—this work; ▲—the difference between α′ determined by NBS and this work; □—thermal expansion of Invar[10]; ——— correction added to α′.

from rapid boil off of He when the heaters are first turned on. The actual extent of this error is dependent upon experimental technique and has been minimized by very low initial heating rates. That portion of the systematic error which is due to the thermal expansion of the equipment has been added to all of the data in this work.

In addition to the systematic deviations just discussed, examination of Figure 3 shows that there is also a random scatter of the expansivity of about $\pm 1 \times 10^{-6}/°\text{K}$. This scatter is most likely due to slight thermal gradients which develop in the equipment and varies from sample to sample and from run to run. Since these deviations cannot be compensated, the resolution is considered to be $\pm 1 \times 10^{-6}/°\text{K}$. Therefore, changes in thermal expansion shall be considered to be significant only if changes in linear thermal expansion are greater than $3 \times 10^{-6}/°\text{K}$.

2.3 Determination of thermal expansivity

Up to this point, it has just been stated that thermal expansion has been obtained from electrical signals which are functions of the length and temperature of the sample. The details of these calculations will now be considered. The linear thermal expansion of a material is defined at constant pressure as $\alpha' = (1/l)\, dl/dT$. From this instrument we obtain neither l nor T directly, but rather $l = l_0 + \text{K}\, L$ in view of our previously stated linearity and $E = f(T)$ where L and E are the voltages of the LVDT and thermocouple signals respectively. We can then write

$$\begin{aligned} \alpha' &= 1/(l_0 + \text{K}L)\,(\text{K}dL/dT) \\ &= 1/(l_0 + \text{K}L)\,(\text{K}dL/dE)\,(dE/dT) \qquad (1) \end{aligned}$$

To evaluate this relationship, we use a value of K obtained from calibrating the LVDT with the micrometer, take the derivative dE/dT from standard tables,[9] and compute values of dL/dE by a least squares technique.[12] This procedure was suggested by the work of previous investigators.[1] The technique involves passing a least squares polynomial through a moving arc of the L vs. E data. From the coefficients of the polynomial dL/dE and thus l and α' are computed. These calculations were carried out on a Univac 1108 computer. The program along with sample data and an explanation of input and output parameters are given in Appendix I of reference 13.

2.4 Experimental procedure

After molding the sample material to thin films (10–20 mil), specimens are cut and mounted in the sample grips with the use of a special jig which insures proper alignment and a nominal sample length of 1.50 inches. The assembly is then examined on an optical comparator to check sample alignment and length (± 0.001″). When the sample has been properly mounted, it is connected to the LVDT by the support tubes and the whole assembly is inserted into the cryostat which is then closed and evacuated for 24 hours prior to cooling down. This insures that the samples all are properly dried. The cryostat is cooled from room temperature to about 85 K overnight by filling the outer Dewar with liquid N_2. Cooling below 100 K is possible only by allowing N_2 exchange gas into the cryostat and into the wall area of the inner Dewar. Final cooling down to 4.2 K is accomplished by adding about 4 liters of liquid He to the inner Dewar, subsequent to evacuating and sealing off the inner Dewar wall. After filling with liquid He, the cryostat is allowed to sit for 1–1.5 hours during which time the helium level falls to about 1″ below the bottom of the sample chamber. This waiting time is necessary to allow the support tubes to reach temperature equilibrium relative to each other.

After proper equilibrium conditions are obtained, the sample is slowly heated ($< 15°$/hr for $T < 20$ K, 30°/hr for $T > 20$ K) by supplying voltage to the heaters. The actual heating rate is determined by the judicious adjustment of a well regulated voltage supply which is equipped with a very fine control. With practice and patience it is possible to control the time required to heat the sample one degree to 120 ± 2 seconds. The voltage of the external heater can be controlled separately and its temperature is maintained to ± 1° of the temperature of the sample well.

Length and temperature readings are taken at regular intervals (usually 1 degree) as the temperature is increased at a constant rate. Under normal conditions the data are collected in three overlapping runs (i.e. 6–120, 95–240, 220–350 K). This technique, although somewhat more time consuming, is found to be superior to one continuous run, for extended runs result in a very large thermal gradient between the sample chamber and the inner Dewar. Invariably this high gradient leads to difficulties in controlling the heating rate. Overlapped data usually yield values of α' within $\pm 2 \times 10^{-6}/°\mathrm{K}$. The data are then analyzed by the techniques mentioned in the previous section.

2.5 Materials

The specimens used in this investigation were all amorphous polymers and are listed in Table I. The samples were cut from thin films (10–20 mils) which had been molded 20–40° above their respective T_g or T_m and then quenched rapidly (45–60 seconds) to the glassy state. These conditions were chosen to insure maximum relaxation effects, to avoid crystallinity in those polymers which can crystallize, and to prevent degradation in those systems which are unstable.

TABLE I

Polymers studied

Polymer	Symbol	Specific volume	Repeat unit
Polystyrene[a]	PS	0.9582	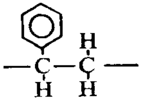
Polyalpha-methyl styrene[a]	PαMS	0.9896	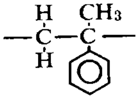
Polyorthmethyl styrene[a]	POMS	0.9807	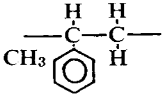
Polycarbonate	PCA	0.8379	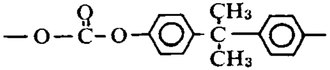
Polyphenylene oxide	PPO	0.9346	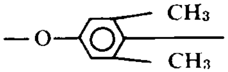
Polycyclohexylene dimethylene[b] terephthalate (cis)	CHDMT	0.8321	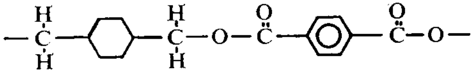
Polyimide	KAPTON	0.6863	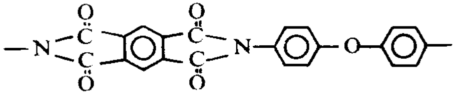

opentyl methacrylate[c]	PC5MA	0.8935	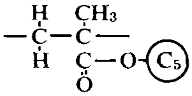
ohexyl methacrylate[c]	PC6MA	0.9064	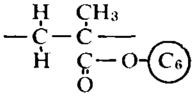
oheptyl methacrylate[c]	PC7MA	0.8956	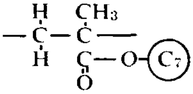
looctyl methacrylate[c]	PC8MA	0.9079	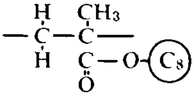
utyl methacrylate	PNBMA	0.9487	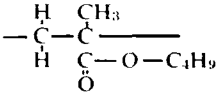
utyl methacrylate	PTBMA	0.9786	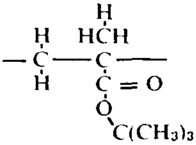

---

ained from R. F. Boyer, Dow Chemical Co.
ained from J. M. Anderson, Case Western Reserve University.
ained from Jo Heijboer, Centraal Laboratorium TNO, Delft, Netherlands.

3 RESULTS AND DISCUSSION

In this section, correlations between relaxations found by dynamic techniques and the dilatometric technique will be explored. It is to be expected that the corresponding relaxations will be found at lower temperatures in the dilatometric data since the dynamic measurements were usually carried out at 1 Hz, whereas the dilatometer usually has a much lower effective frequency (see for example reference 2). The selection of the appropriate frequency-temperature shift of dynamic data to dilatometric frequencies is difficult for two reasons. The primary problem is that the frequency of a dilatometric experiment cannot be measured directly as so many Hz. Therefore, it is said to have an effective frequency based on the temperature shift of relaxations which have a known activation energy. Secondly, for some of the polymers studied there are data available at only one frequency so that it is not possible to determine frequency shift data or the corresponding activation energies.

In this work, a semi-empirical method has been adopted for determining the appropriate temperature-frequency shift of relaxations. This technique is based on a single point method for determining the activation energy of a relaxation process, which has been suggested by Gibala[14] and Heijboer.[15]

Heijboer has calculated the activation energy (ΔH) of γ-relaxations in a series of cycloalkyl methacrylates from the expression

$$\nu = \nu_0 \exp \{-\Delta H / RT_{\max}\} \qquad (2)$$

where ν is the test frequency and $T_{\max}$ the relaxation temperature. Heijboer found that calculated and experimental values of ΔH agreed reasonably well if ν_0 was taken to be 10^{13}, i.e. of the order of a molecular frequency. Table II presents Heijboer's values for the cycloalkyl methacrylate γ-relaxations. Also included are values of ΔH computed using a value of $\nu_0 = 10^{14}$. For two of the three polymers listed, it seems that better agreement is obtained with the

TABLE II

Activation energies of γ relaxations in poly(cyclo-alkylmethacrylates)

Carbon atoms in side ring	Apparent activation energy, Kcal/mole		
	a	b	c
5	—	<4	<4
6	11.5	11.5	12.4
7	6.0 ± 1	5.5	5.9
8	10.5	9.5	10.2

a. From the log ν—1/T diagram.[15]
b. From $\nu_0 = 10^{13} \exp\{-H/RT\}$[15]
c. From $\nu_0 = 10^{14} \exp\{-H/RT\}$ This work

latter value. It remains to be seen whether eq. (2) remains valid for more widely varying relaxation temperatures and processes.

If a single test frequency is adopted and ν_0 is assumed to be constant for all relaxation processes, eq. (2) can be rewritten as

$$\Delta H = RT_{\max} \ln(\nu_0/\nu) = CT_{\max} \tag{3}$$

where C is a universal constant for a given frequency ν. This is the form suggested by Gibala.[14] To test this idea, two curves were constructed in which activation energies are plotted as a function of temperature at 1 and 0.01 Hz for various sub-T_g relaxations. The results are exhibited in Table III and Figure 4. Since they have been obtained by several authors who used various techniques, we feel that the fit found in Figure 4 is very satisfactory. The lines through the data represent values of C of 65 and 75 cal/mole/degree for 1 and 0.01 Hz respectively. Using eq. (2) and a ν_0 of 10^{14} one obtains slopes of 64.0 and 73.2 respectively for 1 and 0.01 Hz. Heijboer has assumed $\nu_0 = 10^{13}$ which gives the somewhat lower values for C of 59.5 and 68.7 for the same frequencies. A comparison of the two curves in Figure 4 shows that a relaxation of 0.01 Hz occurs at a temperature which is 86.7% of that of the

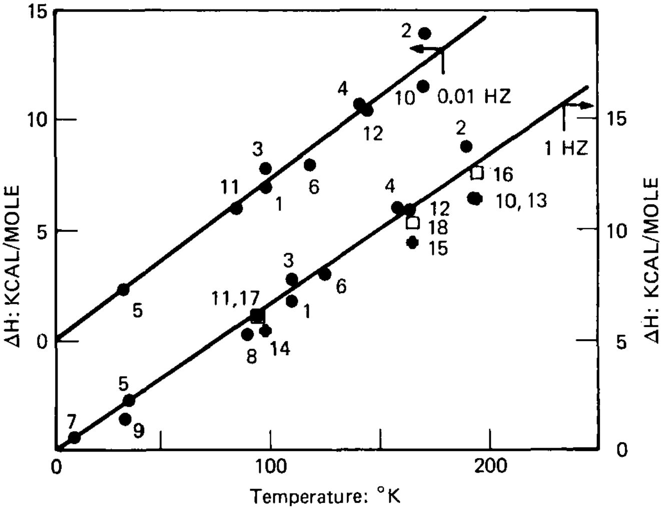

FIGURE 4 Activation energy as a function of temperature at 0.01 Hz and 1 Hz. ○—Experimental; +—Calculated by Heijboer (see Table II); □—This work (Table II).
1—PVnBE; 2—PVnBE; 3—PVME; 4—PVME; 5—PS; 6—PPro; 7—P4MP1; 8—P4MP1; 9—PEMA; 10—PC6MA; 11—PC6MA; 12—PC8MA; 13—PC6MA; 14—PC7MA; 15—PC8MA; 16—PC6MA; 17—PC7MA; 18—PC8MA.

TABLE III

Estimated activation energy and relaxation temperature from one-point method

Polymer	Symbol	Experimental $T_{1\,\mathrm{Hz}}$	Experimental $T_{0.01\,\mathrm{Hz}}$	Calculated $T_{0.01\,\mathrm{Hz}}$	Experimental ΔH	Estimated ΔH	Reference
Poly(vinyl n-butyl ether)	PVnBE	111	98	98	6.9	7.2	2
		189	169	165	13.8	12.3	2
Poly(vinyl) methylether)	PVME	110	97	98	7.7	7.1	2
		162	141	142	10.7	11.5	2
Polystyrene	PS	35	33	33	2.3	2.3	16
Poly(propylene oxide)	PPrO	125	118	110	7.9	8.1	16
Poly(4-methyl pentene-1)	P4MP1	11			0.4	0.7	16
		96			5.2	5.8	16
Poly(ethyl methacrylate)	PEMA	34			1.5	0.7	16
	PC5MA	60			<4	3.9	15
	PC6MA	194	170	170	11.5	12.6	15
	PC7MA	94	83	84	6.0	6.1	15
	PC8MA	163	143	142	10.5	10.6	15

temperature for the 1 Hz relaxation. This is obtained from the relationship

$$\begin{aligned} T(0.01\ \text{Hz}) &= [C(1\ \text{Hz})/C(0.01\ \text{Hz})] \times T(1\ \text{Hz}) \\ &= 0.867 \times T(1\ \text{Hz}) \end{aligned} \tag{4}$$

For the values of C obtained from eq. (2) with $\nu_0 = 10^{14}$, one has;

$$T(0.01\ \text{Hz}) = 0.874\, T(1\ \text{Hz})$$

Equation (4) was tested by calculating the relaxation temperatures at 0.01 Hz from 1 Hz data and comparing the results with experimental data, as is seen in Table III and Figure 5. This figure indicates that the estimation of the relaxation temperature is rather good for the sub-T_g relaxations given. The γ-relaxation in poly(dl-propylene oxide) shows the maximum deviation of about 10%.

It is certainly noteworthy that the rate expression, eq. (2), with a nearly universal value of the pre-exponential factor or the entropy of activation, should describe the behavior of such diverse polymers in different relaxation regions. Cooperativity in the relaxation process might provide a possible rationalization of this general feature.

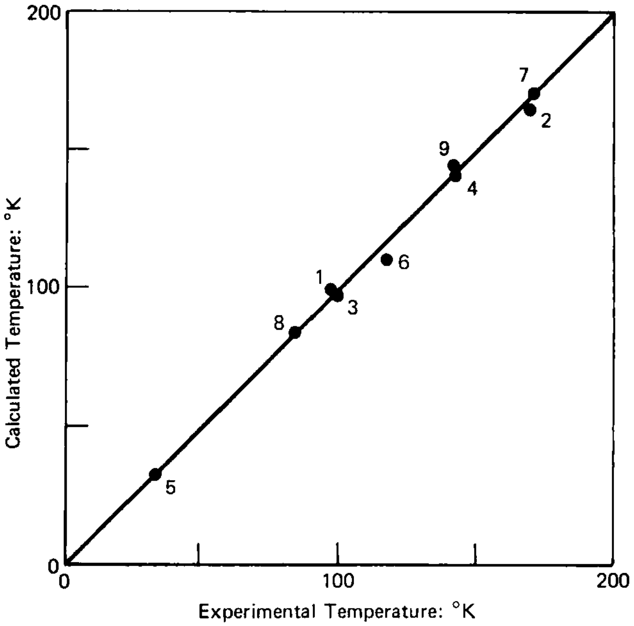

FIGURE 5 Comparison of experimental relaxation temperature at 0.01 Hz with temperatures predicted for 1 Hz data by Equation 3. 1—PVnBE; 2—PVnBE; 3—PVME; 4—PVME; 5—PS; 6—PPro; 7—PC6MA; 8—PC7MA; 9—PC8MA.

For what follows it is desirable to establish a relationship between relaxation temperatures derived from thermal expansivities and from dynamic moduli (granting such a correspondence exists; see below). Figure 6 illustrates such a relationship for those of our polymers in Table I for which the requisite experimental information is available, as shown subsequently. The equation of the solid straight line is: $T(\alpha) = 0.8 \times T(1\ \mathrm{Hz})$. Substitution into eq. (2) with $\nu_0 = 10^{14}$ Hz leads to an effective dilatometric frequency of $10^{-3.8}$ Hz. As will be noted in Figure 6, the result is insensitive to the exact frequency assignment.

In Table IV are shown the computed and observed relaxation temperatures, the latter to be documented in subsequent graphs. The gaps in the $T(\alpha)$ column result from either undetectably small changes in α or location of $T(\alpha)$ in the "third law" region.

3.1 Cryogenic dilatometry and internal friction results

By chemical structure, the polymers investigated (see Table I) fall naturally into three categories and will be thus grouped for discussion purposes. In

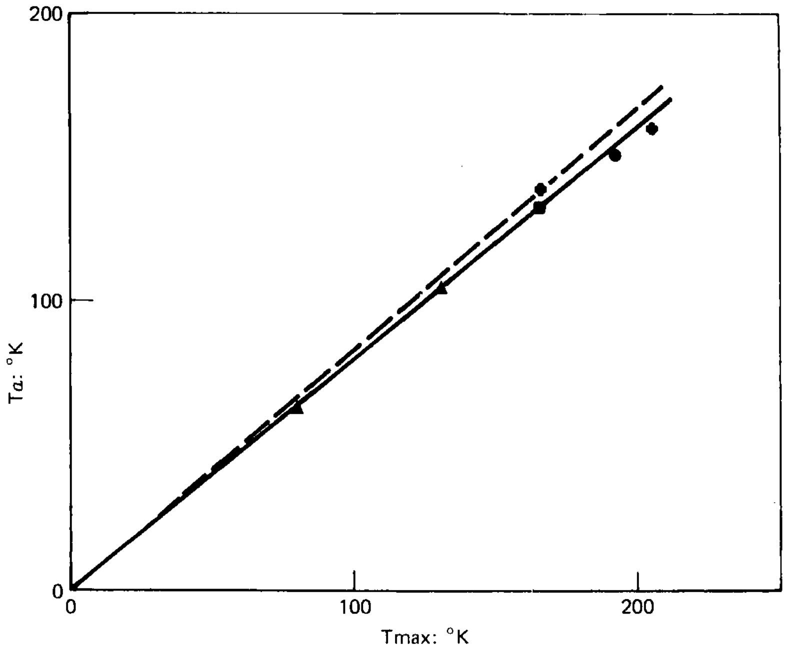

FIGURE 6 Correlation between dynamic relaxation at 1 Hz and Tα. ×—PCA; +—CHDNT; ●—PC6MA; ○—PC7MA; ■—PC8MA; ▲—PαMS; ——— calculated assuming $\nu = 10^{-3.8}$ Hz; --- —— $\nu = 10^{-3}$ Hz.

TABLE IV

Correlation of dynamic and dilatometric relaxations

Polymer	T(1 Hz)	$T(\alpha)$	T ($10^{-3.8}$ Hz)
PS	40	—	32
PαMS	130	105	104
POMS	35	—	28
PCA	165	139	132
CHDMT	205	160	164
CHDMT	100	—	80
PPO	80	65	64
PPO	12	—	10
KAPTON	180	—	144
PC5MA	60	—	48
PC6MA	193	151	154
PC7MA	94	72	75
PC8MA	163	133	131

those cases where internal friction data are available, significant changes in α' will be correlated with relaxations which have been detected by dynamic mechanical methods. Mechanical relaxations have been attributed to various molecular species in various polymers and have been shown to be sensitive to the thermal history of the polymer involved (see for example reference 17). This work will again show that sub-T_g relaxations can be detected by a dilatometric technique and that their location and intensity are functions of molecular structure.

Figure 7 is a schematic representation of the thermal expansion behavior of three hypothetical polymers. Curve A represents a polymer which has no secondary relaxations below the glass transition. The thermal expansion of such a system is characterized by a single feature which is the pronounced decrease in α as the temperature approaches zero. This feature has been seen without exception in all of the polymers examined in this work as well as those previously studied[4,6] and it has also been observed in metals. This phenomenon will generally be referred to as the third law effect. Martin *et al.* anticipated this behavior in their early work with PS and PMMA and gave a thermodynamic explanation.[18]

Curve B represents a polymer which has a relaxation in the intermediate temperature range ($100 < T < 200$ K). In this case, an onset of increased molecular mobility, which might be indicated by a maximum in internal friction, results in an increase in the thermal expansion (α). If the relaxation occurs at sufficiently low temperatures, the increase in α appears to be a continuation of the third law effect and resolution becomes impossible. This is illustrated by Curve C. Since the materials which have been examined in this study all have relaxations below T_g, only types B and C behavior are to be

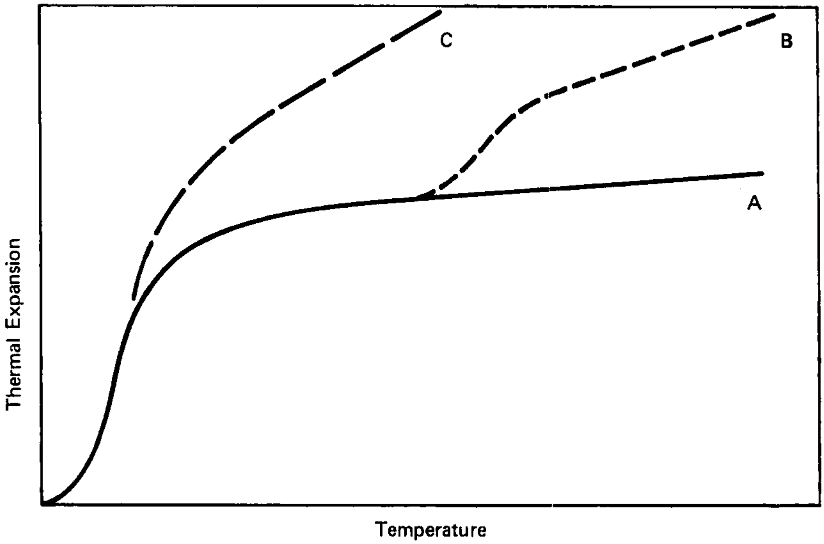

FIGURE 7 Three hypothetical thermal expansion curves. A no relaxations, B one relaxation well above the third law region, C a relaxation in the third law region.

expected. Deviations from type A behavior will be considered to be evidence of the existence of relaxations.

The polystyrene family, here represented by polystyrene (PS), poly(alphamethyl styrene) (PαMS) and poly(orthomethyl styrene) (POMS), will be considered first. The linear thermal expansion (α') and internal friction (Δ) of PS, PαMS and POMS are shown in Figures 8, 9 and 10 respectively.

Figure 8 compares the current results with the work of other authors. The data furnished by Quach *et al.* most closely duplicate these results as they should, since both sets of data were obtained on the same equipment and on material from the same source.[19] The small differences, maximally 5%, may well be due to the fact that Quach made measurements on well annealed samples, whereas our specimens were rapidly quenched. It is now well established that the position and magnitude of dynamic relaxations are a function of polymer history and Haldon and Simha have shown that the thermal expansion of a polymer may be changed by as much as 24% by annealing.[3] The greater variation with the data of Zakin *et al.* might be due to differences in polymer source or thermal history.[1]

Wilson[20] has recently demonstrated the usefulness of the function $d\alpha/dT$ for pinpointing relaxations which might be passed over in examination of only α-T data. Therefore the derivative $d\alpha'/dT$ has plotted as a function of T. Based on the random error of $\pm 1 \times 10^{-6}$ $(°\mathrm{K})^{-1}$ which was observed in the

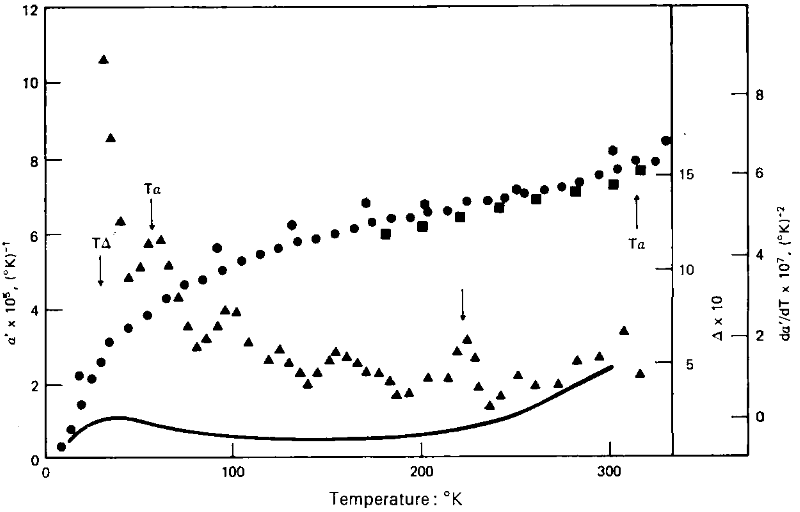

FIGURE 8 Linear thermal expansion, dα'/dT and log decrement of PS. ●—α'; ■—Quach; ◆—Zakin; ▲—dα'/dT,—log decrement.

copper data shown in Figure 3, the criterion for a definite relaxation will be a step in α' of 3×10^{-6} $(°K)^{-1}$. These transitions will be marked with an arrow labeled *Tα*. However, each maximum in $d\alpha'/dT$ has been examined and steps in α' of greater than 1×10^{-6} $(°K)^{-1}$ will be marked with vertical arrows to designate a region of possible relaxation. In Figures 8 to 18, the random error is equal to the diameter of the data points.

In PS we note a sharp increase in thermal expansion in the temperature range 10–45 K followed by a more gradual increase for $50 < T < 280$ K. The sharp increase in α' at the low temperature should be largely due to the third law effect. However, as shown in Figure 8, PS has a dynamic mechanical relaxation at about 40 K and 1 Hz, which should shift to 32 K (marked by *TΔ*) at the dilatometric frequency. This relaxation which has been attributed to the reorientation and wagging of the phenyl group[16,22] probably has some effect on the thermal expansion of PS. This is supported by the fact that PS has a 25% greater α' at 50 K than PαMS or CHDMT which are virtually inactive dynamically in this temperature region.

A pronounced increase in α' is noted in the temperature region 280–315 K. Martin *et al.* noted a similar behavior using both volume and interferometer dilatometers.[18] Figure 8 shows that Quach and Simha also observed this behavior at slightly higher temperatures.[19] We believe that the temperature shift is due to variations in thermal history. The β relaxation in polystyrene has been reported to occur in this temperature region.[23]

There are two additional maxima in $d\alpha'/dT$ which stand out above the scatter. These occur at 58 and 220 K and correspond to increases in α' in the range of 1–3 × 10^{-6} (°K)$^{-1}$. Such small steps may be considered as "possible" relaxation regions and will be thus marked with a plain vertical arrow.

Figure 9 shows that PαMS has a slight increase in α' centered at $T\alpha = 105$ K. This agrees well with the dynamic peak which would be predicted at $T\Delta = 104$ for $10^{-3.8}$ Hz. There is a corresponding broad maximum in $d\alpha'/dT$ spanning the range of 74–130 K. Above 280 there is a gradual increase in α', also reflected in $d\alpha'/dT$. Although the dynamic relaxation in PαMS at 130 is nearly as intense as the δ-relaxation in PS, the effect on α' is much less, possibly due to its higher temperature (see the following section).

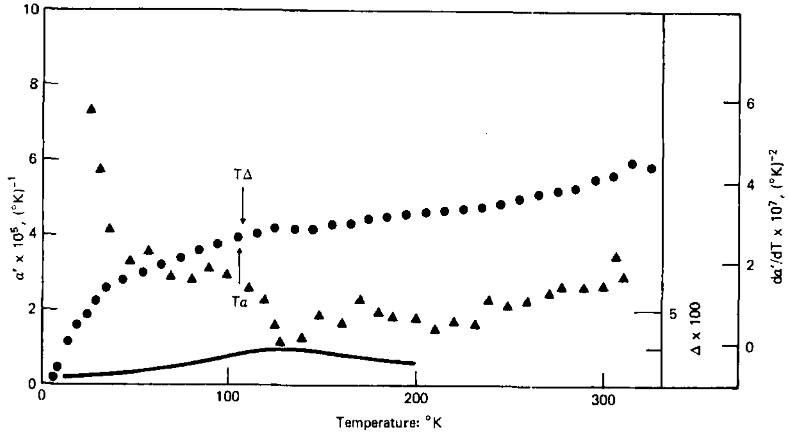

FIGURE 9 Linear thermal expansion, $d\alpha'/dT$ and log decrement of PαMS. ●—α'; ▲—$d\alpha'/dT$; —— log decrement.[16]

The thermal expansion of POMS shown in Figure 10, has two features which distinguish it from the other two styrene polymers. In the very low temperature region α' increases sharply, remains constant for nearly 30 degrees and then rises sharply again between 60 and 70 K. Above 80, POMS behaves much like PS in the region where no relaxations occur. Because of the unusual behavior in the region $T < 70$ K, there has been some concern that the data may be in error. However, the more conventionally shaped curve depicted by the broken line, would require unexplained experimental errors far in excess of any observed in other systems. Therefore we believe that this behavior must be caused by the low temperature relaxations which occur in POMS. The largest of these, which is due to the rotation of the phenyl ring, would be expected around 28 K at dilatometric frequencies (see Table IV). This agrees only moderately well with the dilatometric relaxation which is estimated from

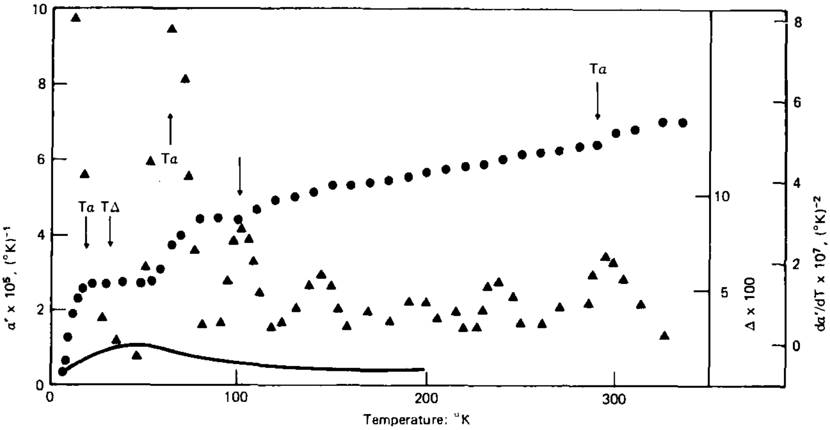

FIGURE 10 Linear thermal expansion, $d\alpha'/dT$ and log decrement of POMS. ●—α'; $d\alpha'/dT_0$; —— log decrement.[16]

the maximum deviation between the data and the broken line to occur at 20 K This relaxation is stated to occur at a lower temperature in POMS than in PS, since the unsymmetrical ring allows a simpler distinguishable motion.[24] High frequency dynamic measurements show that POMS also has a relaxation process which would occur below 10 K even at 1 Hz. This relaxation is most likely due to the methyl group in POMS. The peculiar behavior of α' noted in POMS has also been seen in other polymers and by other investigators. This will be discussed later in Section 3.3.

The second feature in POMS is the small but distinct increase in expansivity at 295 K. This relaxation is near the limit of resolution of this equipment but it is felt that the effect is real because it is very sharp and appeared on duplicate runs.

Two further maxima in $d\alpha'/dT$ are noted at 60 and 102 K, both being beyond experimental uncertainty. Neither of these have corresponding dynamic relaxations and remain unexplained.

The second group consists of four amorphous polymers which are known to be tough as much as 270 K below their respective glass transition temperatures. In previous work,[25,26] it was shown that changes in failure mechanism could be related to molecular mobility as evidenced by the level of mechanical damping. Therefore, we wanted to explore whether these systems exhibit a volume-temperature behavior which would be characteristically different from that displayed by the more brittle polymers such as the styrenes or methacrylates.

The first material to be studied was polycarbonate (PCA), shown in Figure 11. The most striking feature is the broad relaxation which appears in both

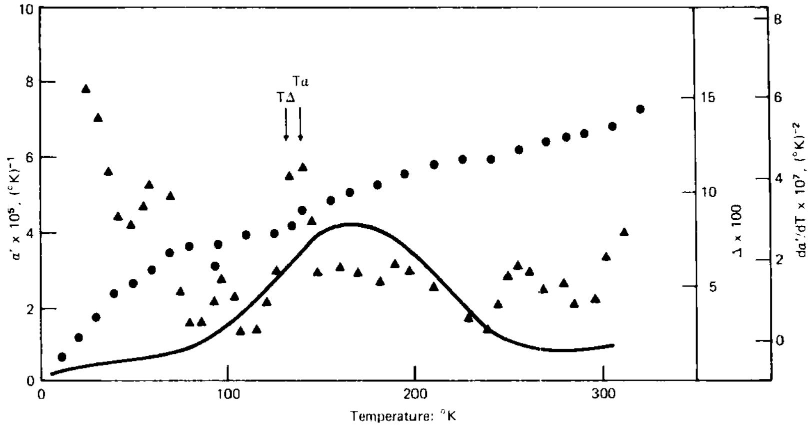

FIGURE 11 Linear thermal expansion, $d\alpha'/dT$ and log decrement of PCA. ●—α'; ▲—$d\alpha'/dT$; —— log decrement.[25,28]

dynamic and dilatometric data. $T\alpha$ and $T\Delta$ are respectively 139 and 132 K, a fair agreement. The $d\alpha'/dT$ curve shows that the large γ-relaxation is actually made up of an intense and narrow peak at 139 and a broad maximum between 150 and 220 K. At 65 K there is a weak maximum which correlates with the onset of the γ-relaxation at 80 K. Near 300 K there is a general increase in $d\alpha'/dT$ which may be due to the β-relaxation reported at 350.[34]

At low temperatures, PCA has a low thermal expansion compared to PS. This is due to the lack of a substantial δ-relaxation in PCA. Perhaps the most surprising feature of the expansivity spectra of PCA is the relatively weak response to the large γ-relaxation.

The second engineering plastic is CHDMT. This material was selected not only because it is tough far below its T_g ($\simeq$ 493 K), but also because it has a low level of mechanical damping below 100 K. This makes it a possible model for polymer systems which behave "ideally" (i.e. no relaxations) at low temperatures. The pertinent data are shown in Figure 12. As in the case of PCA, CHDMT has a low level of thermal expansion below 100 K. The dilatometer yields a relaxation at $T\alpha = 160$ K which agrees well with the calculated value of $T\Delta = 164$ K. Again the γ-relaxation appears to be decomposable into two peaks. There is also the indication in α' of a relaxation at 60 K. As in PCA, the increase in α' at the γ-relaxation is relatively small when contrasted with the large increase associated with the relaxations in the methacrylate polymers.[3,4]

The third tough polymer is polyphenylene oxide (PPO), see Figure 13. As in the case of POMS, the thermal expansion of PPO rises sharply in the temperature range $T < 35$ K, followed by a flatter region and then a second

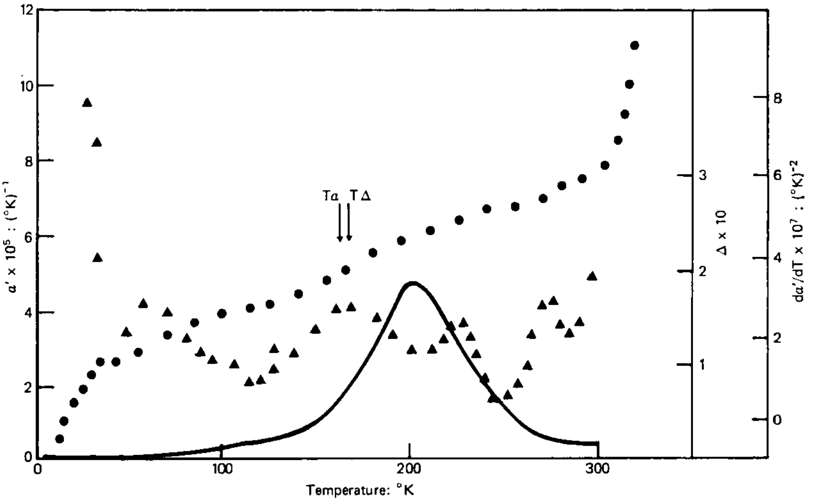

FIGURE 12 Linear thermal expansion, $d\alpha'/dT$ and log decrement of CHDMT. ●—α'; ▲—$d\alpha'/dT$; —— log decrement.[27]

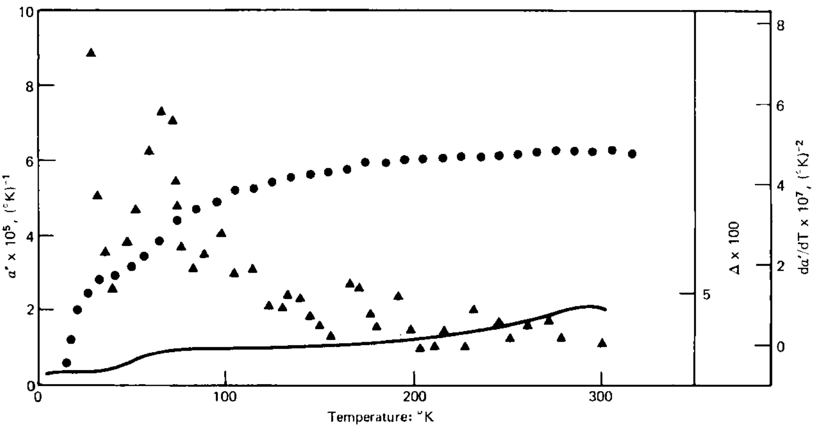

FIGURE 13 Linear thermal expansion, $d\alpha'/dT$ and log decrement of PPO. ●—α'; ▲—$d\alpha'/dT$; —— log decrement.[25,28]

increase in the region $50 < T < 75$ K. This second increase corresponds to a relaxation at 80 K which has been found by internal friction techniques.[25,26] Again the agreement between $T\alpha$ (65) and $T\Delta$ (64) is very good. Above 80 K, the thermal expansion of PPO increases slowly and uneventfully to 300 K, even though dynamic mechanical measurements indicate that this material has a relaxation at 290 K. The α-derivative only emphasizes the lack of activity in this polymer.

Figure 14 shows the thermal expansion and mechanical spectra[26] of Kapton, the fourth tough amorphous material to be examined. This polymer shows no signs of a sharp increase in α' which could be correlated with known relaxation behavior. However, this is not surprising since the relaxation in Kapton is rather weak. The most unique aspect of the thermal expansion is its very low level. It is less than 40% of that of the next lower polymers PαMS and CHDMT.

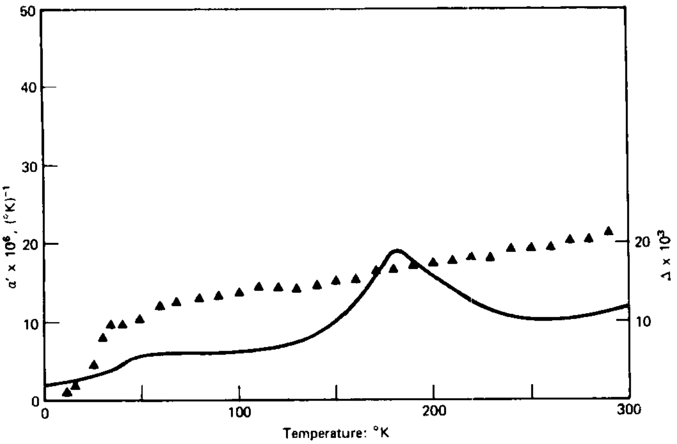

FIGURE 14 Linear thermal expansion and log decrement of KAPTON. ▲—α'/ —— log decrement.

Previous workers have investigated the thermal expansion of a series of esters of poly(methacrylic acid) and have found that the thermal expansivity is a strong function of the side chain alcohol.[3,4] This work was continued by examining the expansivity of four cycloalkyl methacrylates. These materials were found to have high thermal expansions with correlation between the changes in α' and the known mechanical spectra.

Figure 15 shows the mechanical spectra and thermal expansion of poly (cyclopentyl methacrylate). The latter increases rapidly between 10 and 300 K. The initial rise must include the third law effect. In some polymers the rapid rise is followed by a plateau region. However, in the case of PC5MA the low temperature relaxation should be found at $T\Delta = 48$ K at dilatometric frequencies and thus cannot be isolated. The internal friction data by Heijboer on PC5MA suggest the existence of a relaxation somewhere below 100 K.[15] Therefore we measured the log decrement of PC5MA for $4.2 < T < 150$ K. A comparison of Heijboer's and our results indicates some difference in magnitude, which may have resulted from a varied thermal history. Both sets

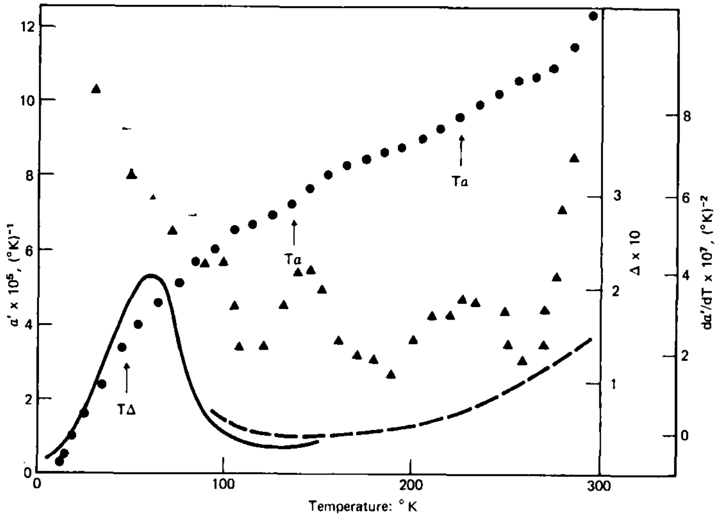

FIGURE 15 Linear thermal expansion, *dα'/dT* and log decrement of PC6MA. ●—*α'*; ▲—*dα'/dT*; —— log decrement.[15]

of measurements indicate that the relaxation is extremely intense considering the low temperature range. This may be the reason it has such a large effect on the thermal expansion behavior.

There are two significant peaks in *dα'/dT* at 140 and 230 K. Although there is no dynamic maximum at the appropriate temperatures, there is a large background damping particularly in the region 250–300 K.

The thermal expansivity of PC6MA is given in Figure 16. Two relaxations at 151 and 75 K are indicated. The former is extremely large and correlates well with the dynamic relaxation at 190 K at 1 Hz.[15] This transition which is due to the cyclohexyl ring would be expected to occur at 154 K at the dilatometric frequency. It should be noted that the relaxation of the cyclohexyl ring is much larger in PC6MA than in CHDMT. It should be further noted that for the 6, 7 and 8 carbon cycloalkyl methacrylates the internal friction is plotted on a reduced scale, as the peaks are very large.

There is a suggestion of a maximum in the log decrement curve below 100 K. This relaxation appears at 75 in the dilatometric data. There are two maxima in *dα'/dT* at 180 and 225 K at the limit of resolution, but may indicate relaxations.

As shown in Figure 17, the thermal expansivity of PC7MA behaves in much the same way as that of PC5MA. That is, it increases throughout the temperature region investigated without a plateau usually associated with the end of the third law effect. This must be due to the relaxation which is centered

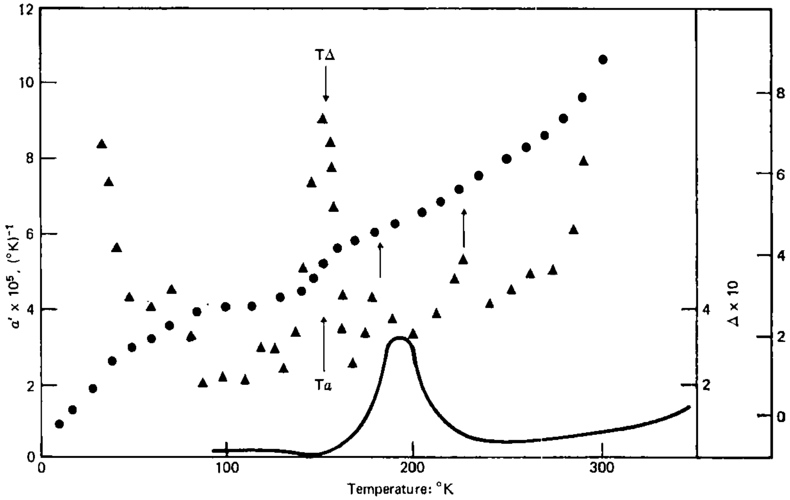

FIGURE 16 Linear thermal expansion, *dα'/dT* and log decrement of PC6MA. ●—α'; ▲—*dα'/dT*; —— log decrement.[15]

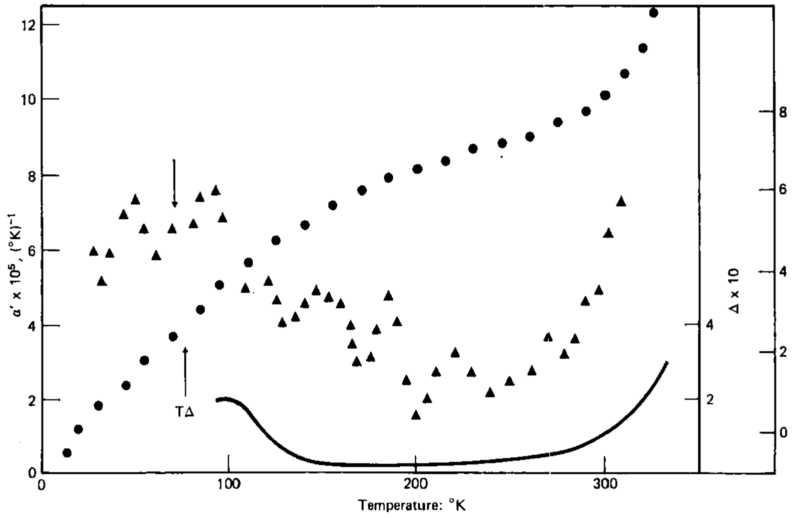

FIGURE 17 Linear thermal expansion, *dα'/dT* and log decrement of PC7MA. ●—α'; ▲—*dα'/dT*; ——log decrement.[15]

at 94 K in the dynamic mechanical spectra. There is a rather broad maximum in $d\alpha'/dT$ from 40 to 105 K and centered around 72 K, which compares favorably with the $T\Delta$ of 75 K for the γ-relaxation.

The thermal expansion of PC8MA is qualitatively similar to that of PC6MA in that both have a plateau region around 100 K followed by a rather sharp increase in α'. As is seen in Figure 18, the sharp increase in α' occurs at about 133 K. This agrees well with a predicted $T\Delta$ of 131 from the dynamic results. The magnitude of this relaxation is very large indicating that the onset of motion of the cyclooctyl ring can cause a large increase in the volume. The temperature derivative indicates that PC8MA has only one major secondary relaxation.

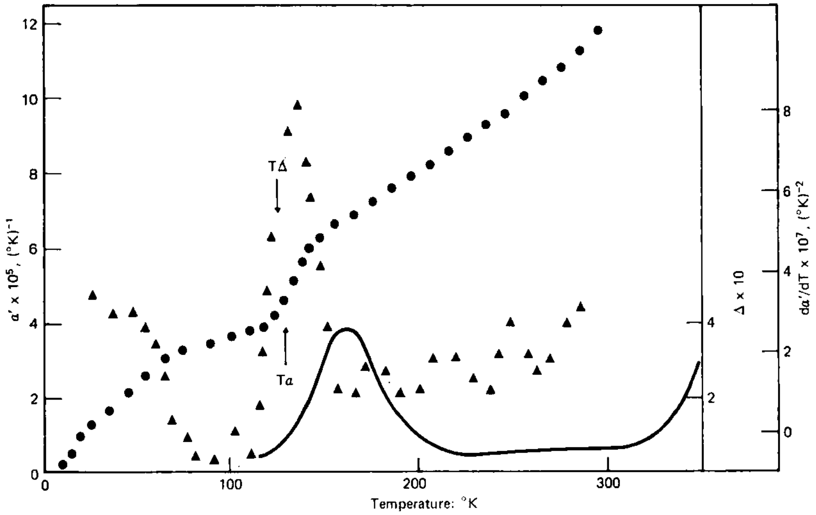

FIGURE 18 Linear thermal expansion, $d\alpha'/dT$ and log decrement of PC8MA. ●—α'; ▲—$d\alpha'/dT$; —— log decrement.[15]

A comparison of the data shown in Figures 8–18 suggests that relaxations (both dynamic and dilatometric) are larger when they originate from pendant groups as opposed to segments of the main chain. In particular, it will be noted that the cyclohexyl relaxations in CHDMT and PC6MA have log decrements of 0.220 and 0.330 respectively, whereas the corresponding changes in α' are 4 and 10 $\times$ 10^{-6} $(°K)^{-1}$. These results indicate that restrictions placed on the cyclohexyl ring as part of the main chain seem to have a greater effect on its contribution to thermal expansion than on its ability to dissipate energy in dynamic shear. It has been suggested that the brittle-ductile transition in CHDMT is related to the large γ-relaxation. Thus a significant change in mechanical properties is accompanied by a relatively small increase in thermal expansivity. This is contrasted by the behavior of PC6MA, with its large increase in α and no noticeable improvement in toughness.[31]

3.2 Effect of dynamic strength and temperature on thermal expansion

It has been pointed out that large relaxations such as those found in the methacrylates caused large changes in α' and that if two dynamic relaxations were to have the same magnitude (as in PS and PαMS), then the lower temperature relaxation has the larger effect on α'. It will be demonstrated that this effect is approximately inversely proportional to its temperature and directly proportional to the internal friction.

We define as excess thermal expansion the difference between the thermal expansion of a given polymer and that of PαMS measured at a point 50 degrees above the temperature at which the relaxation occurs at 1 Hz. PαMS was chosen as the standard since it has the weakest relaxation except for Kapton. The use of PαMS is justified since its α' is similar to that of other polymers below their relaxation region. Since the relaxation effect is proposed to be inversely proportional to the relaxation temperature, the magnitude of the dynamic relaxation has been reduced by dividing by $T_{\max}$. The polymers have been arranged in Table V according to the size of their respective reduced relaxation strengths. A comparison of their excess thermal expansions shows that the empirical rule holds to a first approximation. There are two polymers which are outstanding exceptions to this rule. It should be noted that both PPO and PC6MA have small secondary relaxations which would also contribute to their excess thermal expansion.

TABLE V

Reduced internal friction and excess thermal expansion

Polymer	$\Delta/T_{\max}$	Excess α $\times 10^6$: $(^\circ\mathrm{K})^{-1}$	$\Delta\alpha$ from theory $\times 10^6$: $(^\circ\mathrm{K})^{-1}$
PαMS	0.15	0	12
PPO	0.25 (0.30)†	12	41
POMS	0.49	8	—
PCA	0.51	9	30
PS	0.55	12	25
CHDMT	1.07	15	65
PC6MA	1.68†	25	80
PC5MA	1.79	24	75
PC7MA	2.13	21	80
PC8MA	2.39	31	120
PNBMA	>4.6	29	100

†These polymers have additional secondary relaxations which also contribute to excess α.

An alternative way of defining excess α's which avoids relaxations in the reference system is based on the theoretical expansivities discussed previously.[7,13] This permits the computation of α's for the hypothetical no-relaxation state of a given polymer. The theory is based on the harmonic oscillator approximation for the cell potential but we do not expect the resulting error even at the highest temperatures to affect the trend in the last column. The correspondence between this and the previous column will be noted.

3.3 Very low temperature relaxations

In Figure 10, the thermal expansion of POMS was shown and attention drawn to the characteristic behavior of α' below 80 K. POMS has an extremely low temperature relaxation which has been attributed to its methyl group. It is suggestive to speculate on a connection between this methyl relaxation and the steps in α' for POMS. It is the purpose of this section to give a possible qualitative explanation for the "POMS effect" in hopes that this will be a starting point for future work which might find the ultimate answer.

To test the generality of the "POMS effect", the low temperature thermal expansions of several methyl-containing polymers are compared in Figure 19. The step-plateau-step behavior is very pronounced in POMS and the several PMMA, somewhat less prominent in PPO and nonexistent in PαMS.

Before considering the difference between POMS and PαMS, we suggest the following explanation for this behavior, illustrated in Figure 20. Here the low temperature α' of POMS has been resolved into two additive curves. The lower curve is the type behavior expected from a polymer with no relaxations, and the remainder is the part ascribed to the low temperature relaxation. We assume that the relaxation is caused by the onset of motion of the methyl group and that as each methyl group begins to move it requires an increment of volume. If all of the groups started to move at one temperature, there would be a jump in volume such as occurs at a melting point. This does not happen in a polymer since each methyl group has a slightly different environment and therefore begins to move at different temperatures. Thus the volume increase is spread out over a temperature range of perhaps 20 degrees and there is a resulting maximum in the excess α' associated with the relaxation. For simple groups such as a methyl group the motion is somewhat restricted by the single carbon-carbon bond. Therefore, the motion of the group does not contribute to an increase in α' after the initial effect. A similar type of behavior has been seen in heat capacity measurements for PMMA at 1–5 K and Reese has attributed this excess heat capacity to the motion of methyl groups.[30]

A weak maximum or a plateau in the total observed thermal expansion has been seen at higher temperatures in methacrylates and vinyl ethers. It is

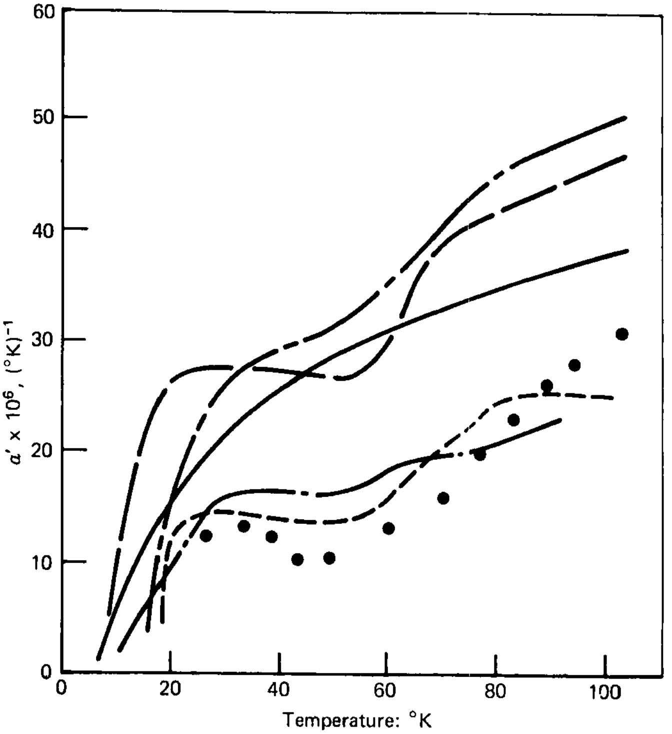

FIGURE 19 Low temperature thermal expansion of methyl containing polymers. ——— ——POMS; ——— PαMS; ——— — ——— PPO; - - - - - - - iPMMA 29; ——— . ——— aPMMA 29; ● PMMA.[4]

unique in POMS and PMMA only in that the effect is so large that it can be observed in the third law region.

Structurally, POMS and PαMS are two similar polymers but Figure 19 shows that their thermal expansivities are vastly different at low temperature, since α' for PαMS drops in the expected monotonic fashion whereas POMS shows the effect of a relaxation. The lack of a similar methyl relaxation in PαMS can best be explained in terms of the relative energy required to rotate a methyl group attached to the main chain as opposed to one on a phenyl group. Sauer[24] has demonstrated by means of model compounds, that rotation of a methyl group is easier when attached to a phenyl ring than to an aliphatic chain. Woodward and his colleagues have shown by NMR that at 10^4 Hz the methyl group rotates in POMS below 77 K while the methyl relaxation occurs at 200 K in PαMS.[31,32] Thus it would seem that the effect of the methyl group is not seen in PαMS simply because it occurs at a higher temperature.

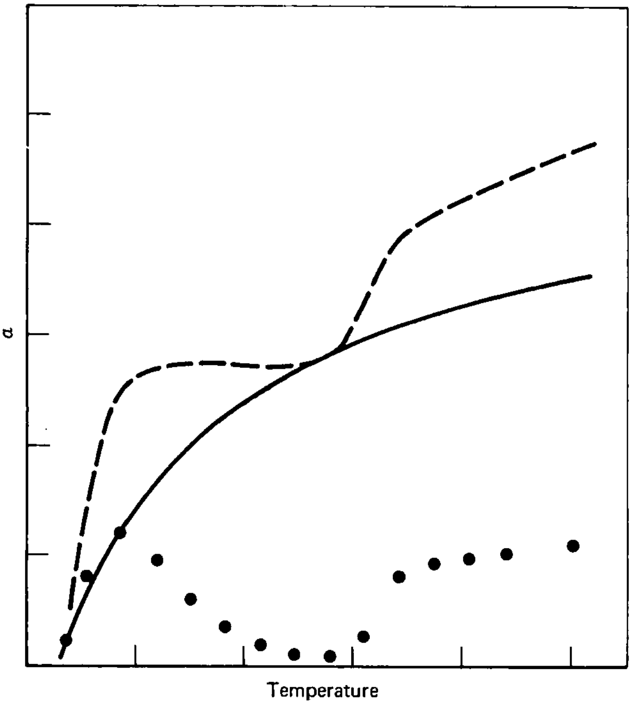

FIGURE 20 Low temperature thermal expansion due to methyl group in POMS. - - - - - - POMS; ——— PαMS (ideal); ●—difference between POMS and PαMS.

3.4 Low temperature equation of state

We have previously compared our experimental results at liquid He temperatures with theoretical predictions.[7,13] These were based on an appropriate modification of the theoretical equation of state developed for the high temperature glass.[33] Satisfactory agreements in the α's ensued up to about 50–70 K, depending upon the relaxations in the respective polymers. At higher temperatures the theoretical α's are uniformly too small. Moreover, the superposition resulting from the appropriateness of a universal value of the reduced quantum temperature $\tilde{\Theta} = 5 \times 10^{-3}$ breaks down. Here we extend the corresponding analysis to polymers studied earlier.[4,6]

At atmospheric pressure the reduced equation of state assumes the form

$$\tilde{\Theta}(\tilde{V}) = \tilde{T} \times \ln \{1 + G(\tilde{V})[2\tilde{V}^{-2}(1.2045-1.0110\,\tilde{V}^{-2})/(3\tilde{\Theta}(\tilde{V})-G(\tilde{V})/2]^{-1}\} \quad (5)$$

where $G(\tilde{V})$ and $\tilde{\Theta}(\tilde{V})$ are explicit functions of the reduced volume.[7] By means of numerical procedures described previously,[13] the reduced volume-temperature curves and hence the $\tilde{\alpha}$–$\tilde{T}$ functions are computed. The latter can then be compared with the experimental data, once the characteristic volume V^* and temperature T^* scaling factors have been determined by appropriate superposition.

Figures 21 and 22 exhibit the reduced expansivities $\tilde{\alpha} = \alpha \times T^*$ as a function of $\tilde{T} = T/T^*$ for alkyl methacrylates, poly(4-methylpentene–1), an ethylene-propylene copolymer,[4] and alkyl vinyl ethers.[6] The theoretical curves are again computed with $\tilde{\Theta} = 5 \times 10^{-3}$. The results are similar to those obtained previously. The principle of corresponding states is satisfied up to $\tilde{T} \simeq 3.5 \times 10^{-3}$. Methyl methacrylate, not shown in Figure 22, exhibits the type of behavior

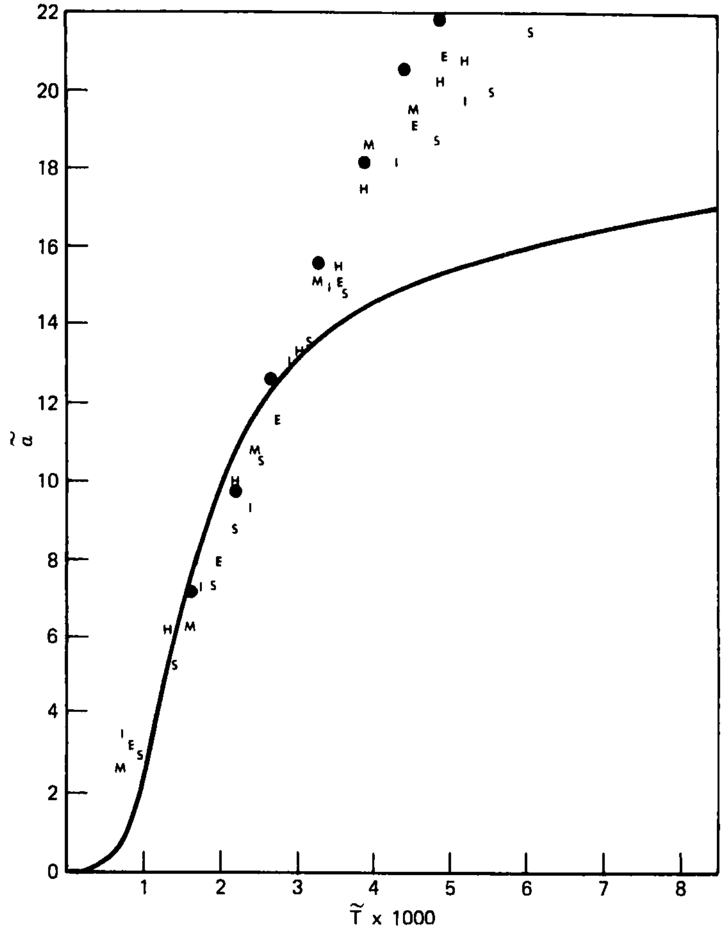

FIGURE 21 Comparison of experimental and theoretical thermal expansion, eq. (5), for poly(vinyl alkyl ethers. M—methyl; E—ethyl; I—isobutyl; S—secondary butyl; H—hexyl; ●—octyl.

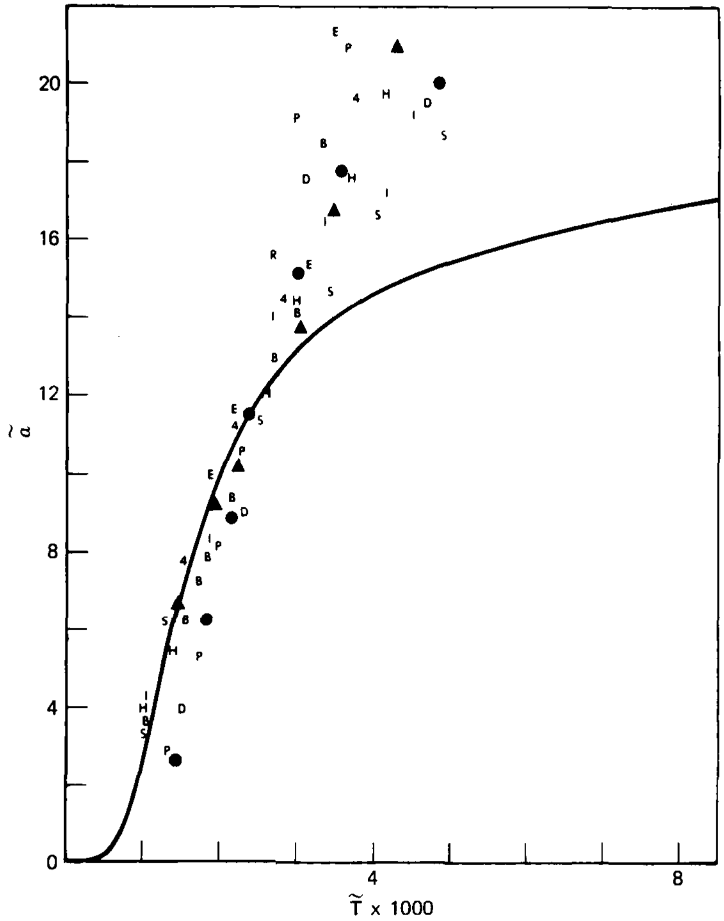

FIGURE 22 Comparison of experimental and theoretical thermal expansion, eq. (5), several poly (alkyl methacrylates) and poly (4-methyl pentene-1) and ethylene-propylene copolymer. ▲—PEMA; P—PnPMA; B—PnBMA; H—PnHMA; O—PnOMA; D—PnDMA; S—PsBMA; I—PiBMA; 4—P4MP1; E—EP.

observed earlier in connection with POMS. On the other hand, the methyl vinyl ether behaves similarly to PαMS and shows no plateau region in Figure 21.

4 CONCLUSIONS

Accurate dilatometry is successful in detecting relaxations which result in changes of not more than 1–3 $\times$ $10^{-6}(K)^{-1}$ in α'. Thus, thermal expansivity serves not only the purpose of studying the equation of state of a polymer in the liquid and glassy states, but also as an important tool in low frequency mechanical relaxation spectroscopy.

The four engineering polymers are seen to have relatively low levels of expansion. Moreover, relaxation processes which are usually associated with their characteristic toughness, are comparatively less active in respect to increases in α'. In contrast, the rather brittle cyclo-methacrylates exhibit large increases in thermal activity on passing through a transition region. Thus, it appears that relaxations resulting from sidechain activity promote an increase in volume but do not improve ductility.

The comparison of Nanda's *et al.* low temperature theory with the earlier measurements of the methacrylate and vinyl ether series leads to the same conclusions as in respect to the present, structurally so different polymers. In particular the same low temperature principle of corresponding states obtains. Exceptions in the low temperature dilatometric pattern occur only in some systems with methyl containing sidegroups.

We conclude with a comment on a basic implication of our results. The theory, eq. (5), rests on an extension of the liquid state cell theory to chain molecular systems. The thermal expansion arises from anharmonicity, determined by the volume dependence of the cell potential. We must conclude that purely vibrational mechanism is not sufficient, even in the glassy state, except at the lowest temperatures, $T \lesssim 50$ K. Above these, a finite temperature dependence of ordering parameters persists.[33,34] Of course, this is also evident from the fact that sub-T_g relaxation processes are detectable by dilatometric methods.

Acknowledgment

We thank the National Science Foundation for support of this work under Grants GK-20653 and GH-36124.

References

1. J. L. Zakin, R. Simha and H. C. Hershey, *J. Appl. Polymer Sci.* **10**, 1455 (1966).
2. R. A. Haldon, W. J. Schell and R. Simha, *J. Macromol. Sci.* **B1**, 759 (1967).
3. R. A. Haldon and R. Simha, *J. Appl. Phys.* **39**, 1890 (1968).
4. R. A. Haldon and R. Simha, *Macromolecules* **1**, 340 (1968).
5. W. J. Schell, R. Simha and J. J. Aklonis, *J. Macromol. Sci.-Chem.* **A3**, 1297 (1969).
6. W. J. Schell, Thesis, Univ. Southern Calif. (1969).
7. R. Simha, J. M. Roe and V. S. Nanda, *J. Appl. Phys.* **39**, 4312 (1972).
8. A. Eisenberg and T. Sasada, in *Physics of Non-crystalline Solids*, J. A. Prins, Ed., North Holland Publishing Co., The Netherlands 1965, p. 99.
9. R. L. Powell, M. D. Bunch and R. J. Corruccini, *Cryogenics* **1**, 139 (1961).
10. T. A. Hahn, *J. Appl. Phys.* **41**, 5096 (1970).
11. A. F. Clark, *Cryogenics* **8**, 282 (1968).

12. A. F. Burmeister, private communication.
13. J. M. Roe, Thesis, Case Western Reserve Univ. (June 1973).
14. R. Gibala, private communication.
15. J. Heijboer, *J. Polymer Sci.* **C16,** 3412 (1968).
16. J. A. Sauer and R. G. Saba, *J. Macromol. Sci.-Chem.* **A3,** 1217 (1969).
17. C. D. Armeniades and Eris Baer, *J. Polym. Sci.* **A2, 9,** 1345 (1971).
18. G. M. Martin, S. S. Rogers and L. Mandelkern, *J. Polymer Sci.* **20,** 579 (1956).
19. A. Quach and R. Simha, *Macromolecules* **4,** 268 (1971).
20. P. S. Wilson, Thesis, Case Western Reserve Univ. (August 1973).
21. C. D. Armeniades, E. Baer and J. K. Rieke, *J. Appl. Polymer Sci.* **14,** 2635 (1970).
22. T. Hara, M. Nozaki and S. Okamoto, Jap. *J. Appl. Phys.* **6,** 1138 (1967).
23. R. F. Boyer, see Table 3, Section Physical Properties—Dynamic Mechanical Loss Spectrum, in *Styrene Polymers*, Encyclopedia of Polymer Science and Technology, N. Bikales, ed. Interscience Publishers, New York (1970).
24. J. A. Sauer, *J. Polym. Sci.* **C32,** 69 (1971).
25. J. M. Roe, M. S. Thesis, Case Western Reserve Univ. (1970).
26. J. M. Roe and E. Baer, *Intern. J. Polymeric Mater.* **1,** 133 (1972).
27. A. Hiltner, private communication.
28. J. M. Roe and E. Baer, *Intern. J. Polymeric Mater.* **1,** 111 (1972).
29. S. Lee, M.S. Thesis, Case 20 RU. (1973).
30. W. Reese, in *Polymers in Space Research*, C. L. Segal, M. Shen and F. N. Kelley, eds., Dekker Inc., New York 1970, p. 221.
31. J. Heijboer, *J. Polym. Sci.* **C16,** 3755 (1968).
32. E. A. W. Hoff, D. W. Robinson and A. H. Willbourn, *J. Polymer Sci.* **18,** 161 (1955).
33. A. Quach and R. Simha, *J. Phys. Chem.* **76,** 416 (1972).
34. T. Somcynsky and R. Simha, *J. Appl. Phys.* **42,** 4545 (1971).